

Fig. 1a. Coronal drawing showing changes in size and shape during normal pneumatization of the maxillary and frontal sinuses.

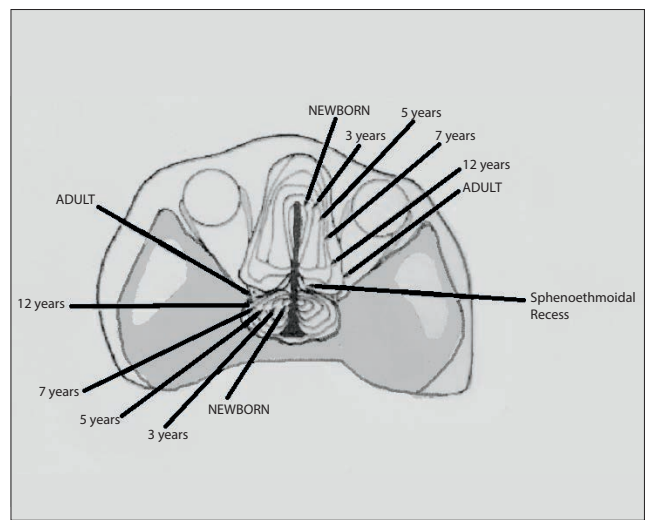


Fig. 1b. Composite axial drawing showing changes in size and shape of the ethmoid and sphenoid sinuses during normal development.

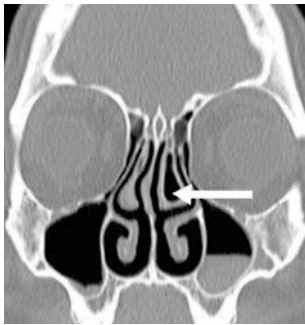


Fig. 2a. Coronal CT demonstrating concha bullosa variant of the left middle turbinate (arrow).



Fig. 2b. Occipitofrontal X-ray demonstrating bilateral agger nasi cells (arrows).



Fig. 2c. Axial CT. Sphenoid pneumatization extends into the left pterygoid process (arrow).

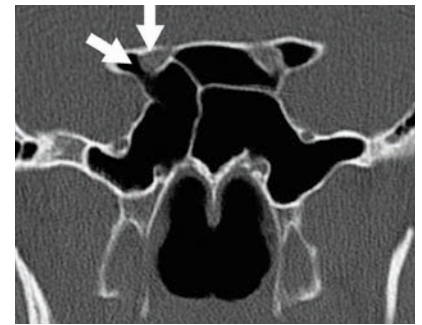


Fig. 2d. Coronal CT demonstrates posterior ethmoid pneumatization extending into the sphenoid sinus creating Onodi cell variant (thin solid arrow). There is aeration of the anterior clinoid processes, with the aerated cavities lying lateral to the optic canal (broad hollow arrow).

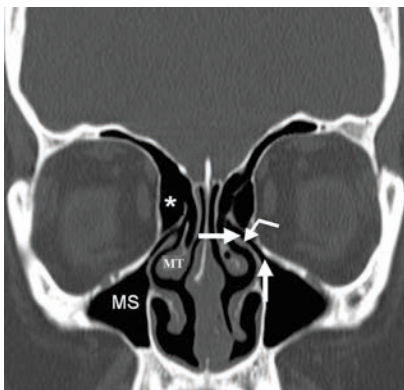


Fig. 3a. Coronal CT of normal ostiomeatal complex (OMC) showing maxillary sinus (MS), middle turbinate (MT), right ethmoid bulla (*), uncinete process (solid arrow), ethmoid infundibulum (curved arrow) and ostium (hollow arrow). The right ethmoid bulla encroaches on the infundibulum.

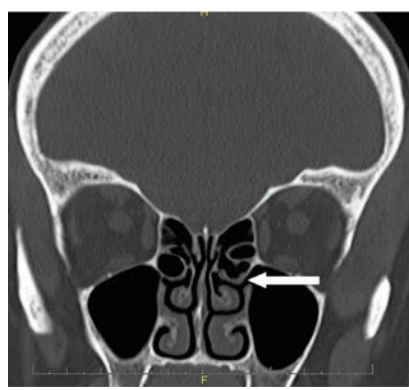


Fig. 3b. Coronal CT demonstrating the left accessory maxillary ostium (arrow).



Fig. 3c. Sagittal CT depicting normal frontal sinus drainage pathway. The frontal sinuses drain via the frontal ostium (short solid arrow) into the frontal recess. The frontal recess communicates with the middle meatus via the hiatus semilunaris (curved arrow). Note the middle turbinate (hollow arrow).

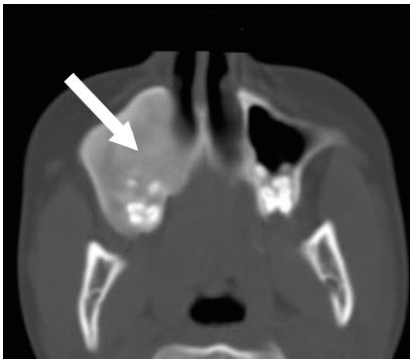


Fig. 4. Axial CT demonstrating fibrous dysplasia of the right maxilla (arrow), and bony expansion of the maxilla with obliteration of the sinus cavity.

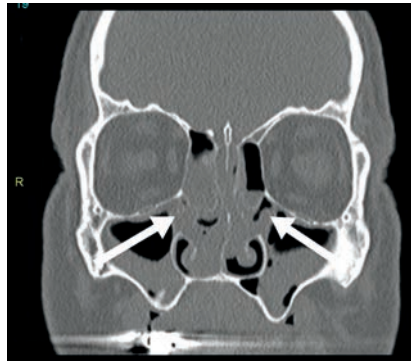


Fig. 5. Coronal CT demonstrating extensive sinonasal polyposis in a patient with cystic fibrosis. Lobulated, mucosal thickening involving the sinuses and nasal cavity with widening of the osteomeatal complexes (arrows) is present.

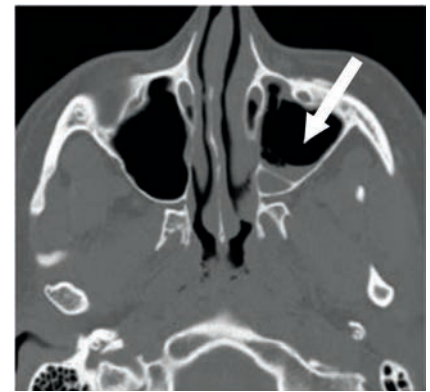


Fig. 6. Acute maxillary sinusitis. CT demonstrates air-fluid level in the left maxillary sinus (arrow).

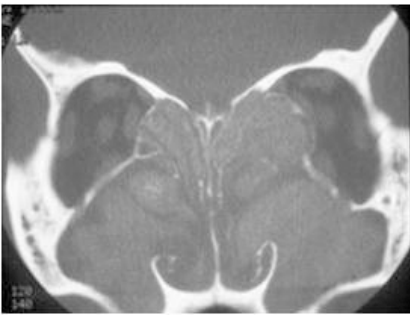


Fig. 7a. Chronic allergic non-invasive fungal sinusitis. Coronal uncontrasted CT depicts the high-attenuation, expansile opacification of the maxillary and ethmoid sinuses. The CT demonstrates the amorphous calcifications, sinus expansion and bony thinning.

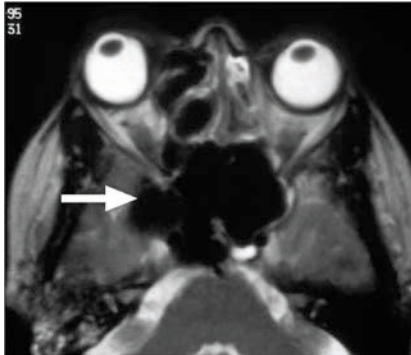


Fig. 7b. Axial T2w MR of fungal sinusitis. There is significant signal loss seen centrally within the opacified sphenoid sinus. The intracranial extension of the fungal sinusitis is demonstrated by the low signal extending into the right middle cranial fossa (arrow).

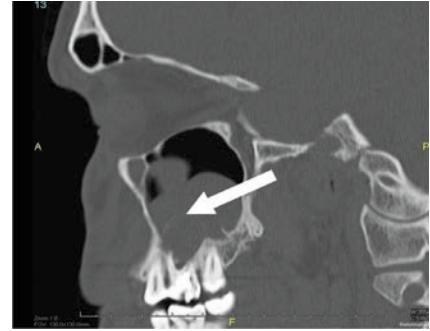


Fig. 8. Sagittal uncontrasted CT reveals radicular cyst with bony remodelling and extension into the maxillary sinus (arrow). The lamina dura of the affected tooth is destroyed. There is sinus opacification secondary to the underlying inflammatory process.



Fig. 9a. Coronal CT demonstrating a mucus retention cyst. A dome-shaped low-attenuation cyst (arrow) is present within the dependant portion of the left maxillary sinus.

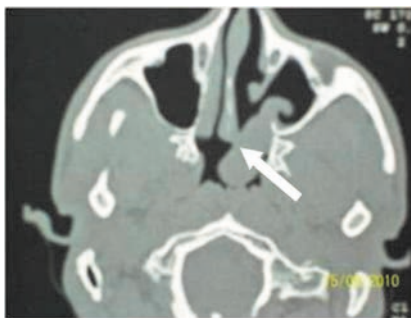


Fig. 9b. Antrochoanal polyp. Axial CT demonstrates a solitary polypoid lesion (arrow) arising from the maxillary antrum widening the sinus ostium and extending posteriorly into the nasopharynx.

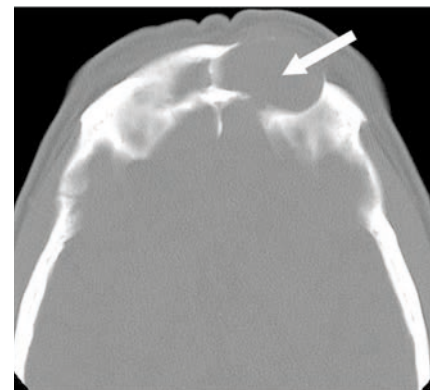


Fig. 9c. Left frontal mucocoele. Axial CT demonstrates a low-attenuation mass expanding the frontal sinus. Bone thinning and remodelling is seen secondary to pressure.

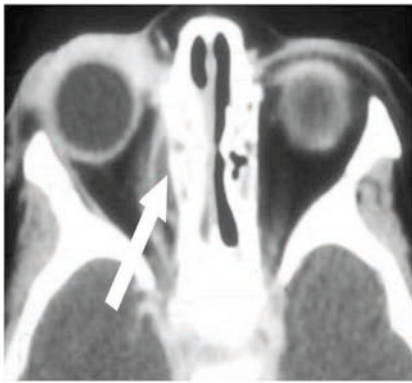


Fig. 10a. Axial enhanced CT of orbits. A subperiosteal abscess is present within right medial extraconal space (arrow). The rim-enhancing abscess displaces the medial rectus muscle.

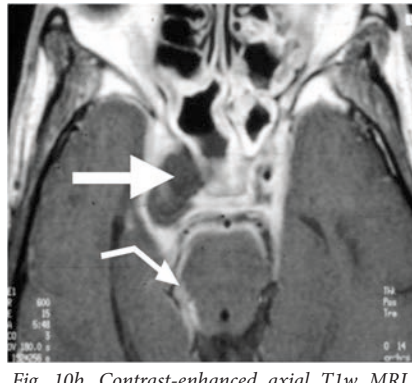


Fig. 10b. Contrast-enhanced axial T1w MRI. Non-enhancing filling defect is seen within expanded right cavernous sinus (arrow). There is loss of flow void within the right internal carotid artery, indicating thrombosis. There is prominent leptomeningeal enhancement surrounding the brainstem, indicating meningitis (curved arrow). An air-fluid level is seen within the right sphenoid sinus.

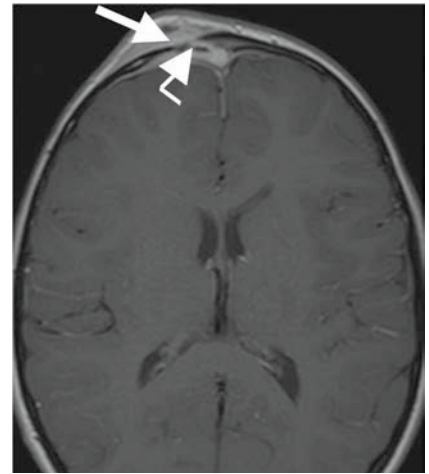


Fig. 11. Pott's puffy tumour. Contrast-enhanced axial T1w MRI demonstrates a rim-enhancing subcutaneous frontal scalp collection (arrow) communicating with osteomyelitis of the frontal bone secondary to frontal sinusitis. There is also a small right frontal empyema (curved arrow).

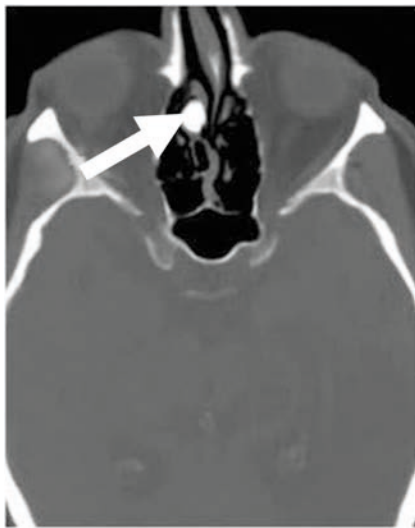


Fig. 12. Right ethmoid osteoma. Axial uncontrasted CT demonstrates well-delineated sclerotic lesion with smooth border (arrow).



Fig. 13. Embryonal rhabdomyosarcoma. Axial contrast-enhanced T1w MRI demonstrates enhancing, aggressive mass arising from sinuses. There is intracranial extension, into the middle cranial fossa (curved arrow). There is also invasion of the right cavernous sinus and right orbit, closely related to the right optic nerve (arrow).

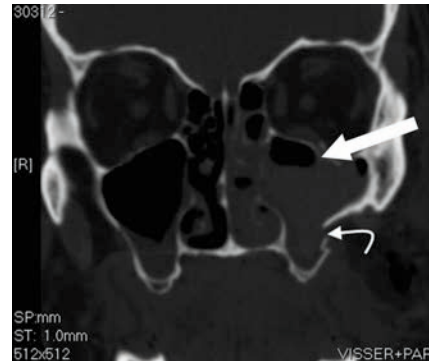


Fig. 14. Blowout fracture. Coronal CT shows fracture of the floor of the left orbit (arrow). There is opacification of the right maxillary sinus and also a fracture of the lateral wall of the sinus (curved arrow).



Fig. 15. Coronal contrast-enhanced T1w MR. Eosinophilic granuloma of the right greater wing of sphenoid (arrow). The adjacent enhancing soft tissue mass encroaches on the maxillary sinus and orbit.



Fig. 17. Axial T2w MRI demonstrating incidental finding of opacified ethmoid air cells in an asymptomatic 4-year-old.

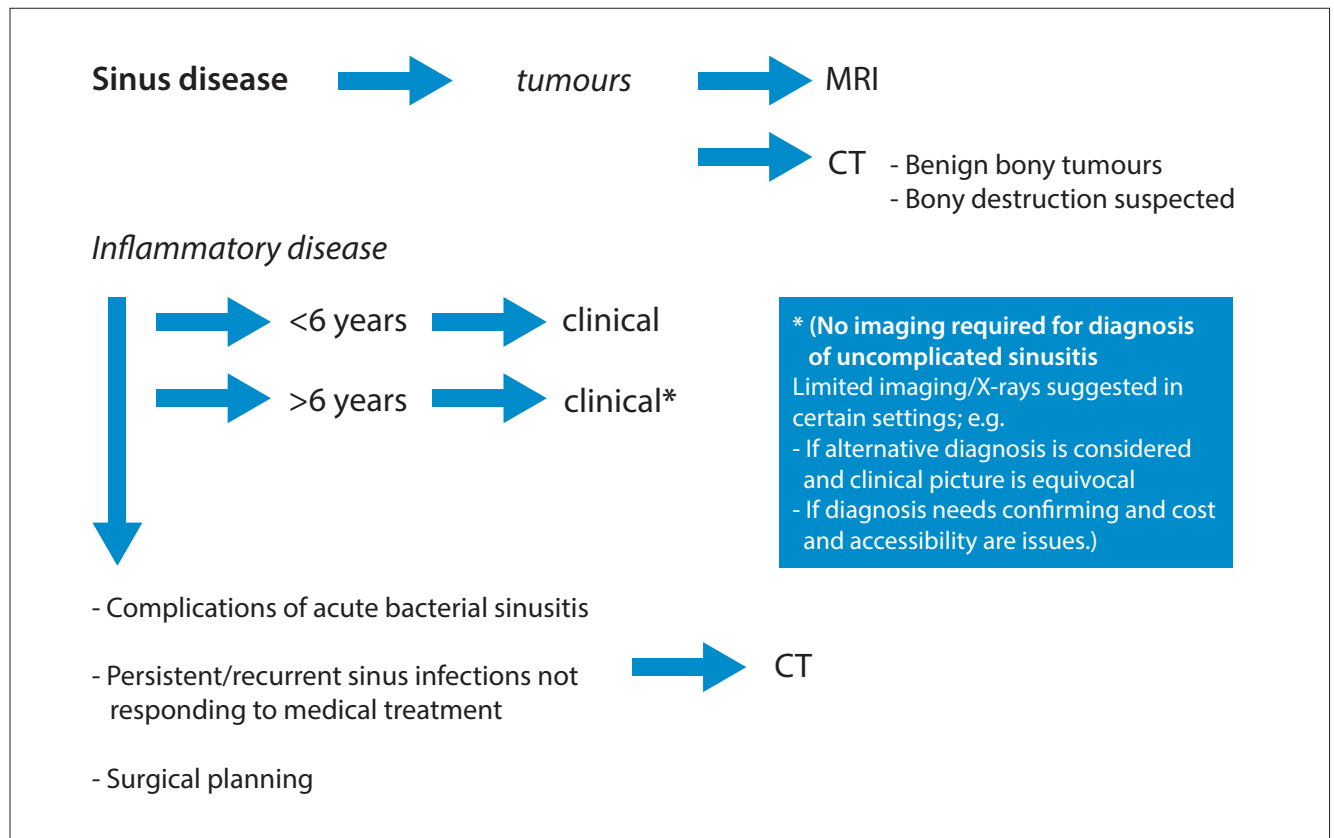


Fig. 16. Proposed algorithm for imaging children with sinus disease.